Nuclear polarization in muonic ^{208}Pb

Akihiro Haga,[1,*] Yataro Horikawa,[2,†] and Yasutoshi Tanaka[1]

[1]*Department of Environmental Technology and Urban Planning, Nagoya Institute of Technology, Gokiso, Nagoya 466-8555, Japan*
[2]*Department of Physics, Juntendo University, Inba-gun, Chiba 270-1695, Japan*

We calculate nuclear-polarization energy shifts in muonic ^{208}Pb. We employ a relativistic field-theoretical calculation and evaluate the ladder, cross, and seagull terms of the two-photon exchange diagrams in both the Feynman and Coulomb gauges. Gauge independence is very well satisfied with the calculated nuclear-polarization energies. Using these results, we analyze fine-structure splitting energies of muonic ^{208}Pb because of the presence of the persisting discrepancies between experiment and calculation. The present nuclear-polarization energies explain about half of the anomaly in the $\Delta 2p$ fine-structure splitting energy, and only one-fourth of the anomaly in the $\Delta 3p$ fine-structure splitting energy.

There is a long-standing problem of the muonic-atom $\Delta 2p$ fine-structure splitting energies. This has arisen from experimental nuclear polarization (NP) extracted from the analysis of muonic ^{208}Pb [1]. The analysis is based on a model-independent nuclear charge distribution from an elastic electron-scattering experiment. Muonic-atom binding energies are then calculated, including various kinds of QED corrections [2]. After adjustment of all corrections other than NP, the difference between calculated and experimental binding energies is interpreted as an experimental NP correction for each muonic level. The experimental NP energies for the muonic $2p$ levels of ^{208}Pb were in disagreement with the theoretical calculation; the calculation predicted a larger NP energy for $2p_{1/2}$ than for $2p_{3/2}$, while the experiment gave a smaller NP energy for $2p_{1/2}$ than for $2p_{3/2}$. The discrepancy in the $\Delta 2p$ energies amounted to 350 eV. In order to clarify this situation, x-ray measurements were carried out at Los Alamos [3] and Paul Scherrer Institute [4]. The measurements did not dissolve the discrepancy. On the contrary, the PSI group has further found the same kind of discrepancies also in the muonic $3p$ levels of ^{208}Pb [4], in the muonic $2p$ levels of ^{90}Zr [5], and in the muonic $2p$ levels of Sn isotopes [6].

Theoretical NP energies employed in the analysis were calculated with only the longitudinal part (the Coulomb part) of the electromagnetic interaction (see, e.g., Ref. [7]). With this interaction, however, a larger NP energy is always predicted for $2p_{1/2}$ than for $2p_{3/2}$, because the $2p_{1/2}$ wave function is closer to the nucleus than $2p_{3/2}$ and thereby has a larger overlap with the transition Coulomb potential. Hence, it is impossible to reproduce the observed tendency of NP energies.

Realizing the fact that the transverse interaction was not negligible in the NP calculation because of the presence of an interference term between the longitudinal and transverse components of the electromagnetic interaction, we calculated NP energies by taking into account the retarded transverse part as well as the longitudinal part of the electromagnetic interaction [8]. We found that the transverse interaction gave rise to NP energies with different muon-spin dependence from those of the longitudinal interaction and one third of the $\Delta 2p$ fine-structure splitting anomaly of muonic ^{208}Pb could be explained by the interference effect.

The calculation of Ref. [8] was based on the noncovariant second-order perturbation theory in the Coulomb gauge. The sum over intermediate nuclear states was carried out explicitly. The sum over intermediate muon states was carried out implicitly using knowledge of the exact muon Hamiltonian, which was equivalent to knowledge of the complete muon spectrum [9]. With this method, however, the photon propagator in the Coulomb gauge could not be properly taken into account. There the retarded effect was estimated by assuming that the energy of the photon propagator was always equal to the excitation energy of the nuclear intermediate state. The transverse parts were neither projected out from the muon nor nuclear currents [10]. Besides, nuclear-polarization corrections of only the ladder diagram of Fig. 1 were evaluated.

The aim of the present paper is to calculate NP energies in the muonic ^{208}Pb by eliminating all deficiencies of the previous calculation. We employ a relativistic field-theoretical treatment of NP calculation presented by Plunien *et al.*, [11] Plunien and Soff, [12] Nefiodov *et al.*, [13] and Haga *et al.* [14] utilizing the concept of effective photon propagators with nuclear-polarization insertions. The formalism allows us to correctly take into account both positive- and negative-energy intermediate states of the muon. The random phase approximation (RPA) is used to describe nuclear transition currents. We evaluate NP energies given by the ladder, cross, and seagull graphs in Fig. 1. (Here, we regard the seagull graph as one of the nuclear-polarization diagrams.) The calculation is carried out in both the Feynman and Coulomb gauges to see how much of the gauge dependence is involved in the results.
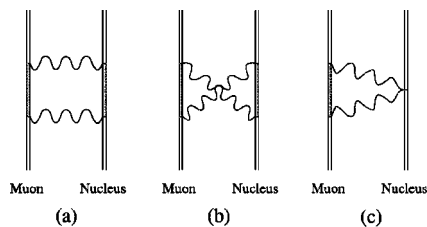
FIG. 1. Diagrams contributing to nuclear polarization in lowest order; (a) ladder, (b) cross, and (c) seagull diagrams.

*Electronic address: haga@npl.kyy.nitech.ac.jp
†Electronic address: horikawa@sakura.juntendo.ac.jp

The nuclear-polarization energy shift due to the ladder and cross diagrams is given by [10,14]

$$\Delta E_{\rm NP} = i(4\pi\alpha)^2 \int d^4x_1 \cdots d^4x_4 \, \bar{\psi}(x_1)$$
$$\times \gamma^\mu S_F^m(x_1,x_2)\gamma^\nu \psi(x_2)$$
$$\times D_{\mu\xi}(x_1,x_3)\Pi_N^{\xi\zeta}(x_3,x_4)D_{\zeta\nu}(x_4,x_2). \qquad (1)$$

Here, ψ is the muon wave function, S_F^m the external-field muon propagator, $D_{\mu\xi}$ the photon propagator in either the Coulomb or Feynman gauge, and $\Pi_N^{\xi\zeta}$ is the nuclear-polarization tensor which contains all information of nuclear dynamics. In terms of transition charge-current densities of j_m^μ and J_N^ξ, the muon and nuclear parts of Eq. (1) are written as

$$\bar{\psi}(x_1)\gamma^\mu S_F^m(x_1,x_2)\gamma^\nu \psi(x_2)$$
$$= \int \frac{dE}{2\pi} e^{-iE(t_1-t_2)} \sum_{i'} \frac{j_m^\mu(\mathbf{x}_1)_{ii'} j_m^\nu(\mathbf{x}_2)_{i'i}}{E - \omega_m + iE_{i'}\epsilon}, \quad (2)$$

$$\Pi_N^{\xi\zeta}(x_3,x_4) = \int \frac{d\omega}{2\pi} e^{-i\omega(t_3-t_4)} \sum_{I'} \left(\frac{J_N^\xi(\mathbf{x}_3)_{II'} J_N^\zeta(\mathbf{x}_4)_{I'I}}{\omega - \omega_N + i\epsilon} \right.$$
$$\left. - \frac{J_N^\zeta(\mathbf{x}_4)_{II'} J_N^\xi(\mathbf{x}_3)_{I'I}}{\omega + \omega_N - i\epsilon} \right), \qquad (3)$$

where $\omega_m = E_{i'} - E_i$ and $\omega_N = E_{I'} - E_I$ are excitation energies of the muon and the nucleus, respectively. The suffixes i and i' stand for the initial and intermediate states of the muon, while I and I' are those of the nucleus.

Performing the integral over the time variable and transferring to the momentum representation, we obtain NP energy shifts for the ladder and cross diagrams,

$$\Delta E_{\rm NP}^L = -i(4\pi\alpha)^2 \int \frac{d\omega}{2\pi} \int \frac{d\mathbf{q}}{(2\pi)^3}$$

$$\times \int \frac{d\mathbf{q}'}{(2\pi)^3} D_{\mu\xi}(\omega,\mathbf{q}) D_{\zeta\nu}(\omega,\mathbf{q}')$$

$$\times \sum_{i'} \frac{j_m^\mu(-\mathbf{q})_{ii'} j_m^\nu(\mathbf{q}')_{i'i}}{\omega + \omega_m - iE_{i'}\epsilon} \sum_{I'} \frac{J_N^\xi(\mathbf{q})_{II'} J_N^\zeta(-\mathbf{q}')_{I'I}}{\omega - \omega_N + i\epsilon}, \quad (4)$$

$$\Delta E_{\rm NP}^X = i(4\pi\alpha)^2 \int \frac{d\omega}{2\pi} \int \frac{d\mathbf{q}}{(2\pi)^3}$$

$$\times \int \frac{d\mathbf{q}'}{(2\pi)^3} D_{\mu\xi}(\omega,\mathbf{q}) D_{\zeta\nu}(\omega,\mathbf{q}')$$

$$\times \sum_{i'} \frac{j_m^\mu(-\mathbf{q})_{ii'} j_m^\nu(\mathbf{q}')_{i'i}}{\omega + \omega_m - iE_{i'}\epsilon} \sum_{I'} \frac{J_N^\zeta(-\mathbf{q}')_{II'} J_N^\xi(\mathbf{q})_{I'I}}{\omega + \omega_N - i\epsilon}. \quad (5)$$

In the present calculation, the nucleus is treated as a nonrelativistic particle. In such a case, the seagull (SG) diagram has to be taken into account to obtain gauge-invariant nuclear-polarization energies. The energy correction due to the seagull diagram is given by [14–16],

$$\Delta E_{\rm NP}^{\rm SG} = -i(4\pi\alpha)^2 \int \frac{d\omega}{2\pi} \int \frac{d\mathbf{q}}{(2\pi)^3}$$

$$\times \int \frac{d\mathbf{q}'}{(2\pi)^3} D_{\mu\xi}(\omega,\mathbf{q}) D_{\zeta\nu}(\omega,\mathbf{q}')$$

$$\times \sum_{i'} \frac{j_m^\mu(-\mathbf{q})_{ii'} j_m^\nu(\mathbf{q}')_{i'i}}{\omega + \omega_m - iE_{i'}\epsilon} \frac{\rho_N(\mathbf{q}-\mathbf{q}')_{II}}{m_p}\delta^{\xi\zeta}. \quad (6)$$

Here, m_p is the proton mass, $\delta^{\xi\zeta}$ the Kronecker delta extended to four dimensions with $\delta^{00}=0$, and $\rho_N(\mathbf{x})_{II}$ is the ground-state charge distribution of the nucleus. The total NP energy shift is given by the sum $\Delta E_{\rm NP}^L + \Delta E_{\rm NP}^X + \Delta E_{\rm NP}^{\rm SG}$. In Eqs. (4), (5), and (6), ω integrations can be carried out analytically as well as angular parts of $\mathbf{q}$ and $\mathbf{q}'$. The formulas for the Feynman and Coulomb gauges are given in Ref. [14].

Dirac muon wave functions are solved in a potential due to a finite charge distribution of ^{208}Pb, which is assumed to be the two-parameter Fermi distribution with $R_0 = 6.6477$ fm and $a = 0.5234$ fm. The nuclear excitations are described by the RPA calculation. The RPA calculation we employed is the same as those performed earlier in Refs. [8,14], i.e., the same harmonic-oscillator single-particle basis, the same particle-hole configuration of approximately a full $3\hbar\omega$ space, and the same Migdal force parameters to describe nuclear two-body interaction. Nuclear transition form factors are calculated by assuming the impulse charge-current operators. In the present calculation, we take into account the nuclear intermediate states with multipolarities 0^+, 1^-, 2^+, 3^-, 4^+, 5^-, and 1^+. For muon intermediate states, we consider the positive-energy states up to 250 MeV including the bound states up to $n \leq 9$ and the negative-energy states down to -250 MeV.

Our nuclear-polarization energies of muonic ^{208}Pb are summarized in Table I. The first column denotes muonic states. The entries in the second column indicate contributions to the NP energy from the ladder, cross, and seagull diagrams. The third column shows NP energies in the Feynman gauge, while the fourth column shows NP energies in the Coulomb gauge. The transverse contributions are included in both columns. The fifth column shows Coulomb NP energies without the transverse contribution (hereafter referred to as CNP). The sixth and seventh columns show results of the previous calculation [8], while the eighth column shows CNP energies calculated in Ref. [7].

Comparison between the results with the Coulomb gauge and those of the Feynman gauge shows that the gauge invariance of NP energy is very well satisfied and the gauge dependence is less than 0.5%. Table I also shows that transverse contributions to NP energies are about 5% for the $1s_{1/2}$ and $2s_{1/2}$ states, 10% for the $2p_{1/2}$ and $3p_{1/2}$ states, and 1% for the $2p_{3/2}$ and $3p_{3/2}$ states, respectively.

Comparison of the present NP energies in the fourth column with those in the sixth column shows that the approximation of Ref. [8] for the retarded interaction is good as far as the magnitudes of the NP energy shifts of the levels are concerned, except for the $1s_{1/2}$ where it overestimates the transverse effect by a factor of 2.

TABLE I. Nuclear-polarization corrections (eV) in muonic ^{208}Pb. Energy shifts ΔE^L, ΔE^X, and ΔE^{SG} are contributions of the ladder, cross, and seagull diagrams, respectively. The abbreviation CNP denotes the unretarded results in the Coulomb gauge.

States	Contribution	Present[a] Feynman (NP)	Present[b] Coulomb (NP)	Present[c] CNP	Ref. [8][d] NP	Ref. [8][e] CNP	Ref. [7][f] CNP
$1s_{1/2}$	ΔE^L	-3783	-4584	-4299	-4806	-4068	-3904
	ΔE^X	-554	$+174$	$+67$			
	ΔE^{SG}	-137	-56				
	Total	-4474	-4466	-4231			
$2s_{1/2}$	ΔE^L	-769	-904	-840	-918	-793	-728
	ΔE^X	-103	$+26$	$+9$			
	ΔE^{SG}	-10	0				
	Total	-882	-878	-831			
$2p_{1/2}$	ΔE^L	-1463	-1727	-1876	-1731	-1855	-1642
	ΔE^X	-226	$+34$	$+17$			
	ΔE^{SG}	$+4$	$+8$				
	Total	-1685	-1685	-1859			
$2p_{3/2}$	ΔE^L	-1427	-1674	-1697	-1666	-1679	-1518
	ΔE^X	-206	$+30$	$+14$			
	ΔE^{SG}	-23	-12				
	Total	-1656	-1656	-1683			
$3p_{1/2}$	ΔE^L	-452	-524	-569	-515	-556	
	ΔE^X	-70	$+9$	$+5$			
	ΔE^{SG}	-20	$+13$				
	Total	-501	-502	-564			
$3p_{3/2}$	ΔE^L	-493	-563	-568	-550	-559	-534
	ΔE^X	-61	$+6$	$+7$			
	ΔE^{SG}	$+1$	$+1$				
	Total	-554	-555	-561			
$3d_{3/2}$	ΔE^L	-201	-227	-255	-231	-253	-232
	ΔE^X	-37	-5	$+0$			
	ΔE^{SG}	$+7$	$+2$				
	Total	-230	-230	-255			
$3d_{5/2}$	ΔE^L	-13	-33	-47	-38	-49	-21
	ΔE^X	-22	-1	$+0$			
	ΔE^{SG}	$+2$	$+1$				
	Total	-34	-33	-47			

[a]Nuclear-polarization energies in the Feynman gauge.

[b]Nuclear-polarization energies in the Coulomb gauge.

[c]The unretarded NP energies in the Coulomb gauge.

[d]Nuclear-polarization energies in the Coulomb gauge. Retarded effects were estimated by assuming that the energy of the photon propagator was equal to the excitation energy of the nuclear intermediate state. Nuclear-polarization correction of only the ladder diagram in Fig. 1 was evaluated. The single-particle nuclear wave functions were solved in a harmonic-oscillator shell model potential.

[e]Same as footnote d except for the unretarded NP energies.

[f]The unretarded NP energies. Same as footnote e except for the single-particle nuclear wave functions in a Woods-Saxon shell model potential.

Our results of CNP are different from those of our previous calculation. The difference comes from the different truncation of nuclear intermediate states, i.e., the intermediate states up to 40 MeV in the present, while those up to 30 MeV in Ref. [8]. Our results of CNP are also different from those of Ref. [7] by about 10%, though the particle-hole space and the particle-hole energies in the RPA calculation are the same in both calculations. The difference may come from different single-particle wave functions, i.e., the former assumes harmonic-oscillator wave functions, while the latter uses Woods-Saxon wave functions. Besides, renormalized electromagnetic transition operators were used in the latter.

We are now in a position to analyze the $\Delta 2p$ and $\Delta 3p$ fine-structure splitting energies of muonic ^{208}Pb using the NP energies given above. Figures 2(a) and 2(b) show how much of the discrepancies are resolved by the present NP calculation. Shaded areas in these figures show the experimentally allowable region of the NP corrections. White circles display results of the CNP, while black circles show results of the NP energies calculated with the full electromagnetic interaction. The transverse interaction gives 147 and 56 eV shifts for $\Delta 2p$ and $\Delta 3p$, which are compared with 111 and 32 eV, respectively, of the previous calculation. As seen from Table I, the cross and seagull diagrams, which
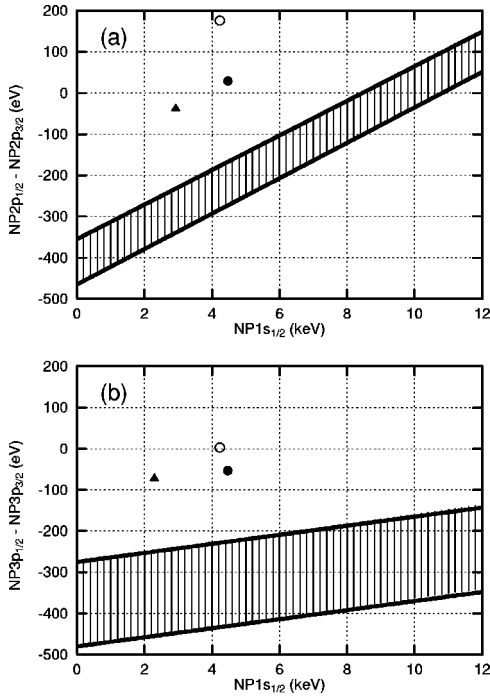
FIG. 2. Nuclear-polarization energy shifts of the muonic (a) $2p$ and (b) $3p$ levels of ^{208}Pb. The shaded area displays experimentally allowable NP energies from Ref. [4]. Calculated Coulomb NP energies are given by white circles, while calculated NP energies are given by black circles. Black triangles are calculated NP plus VP-NP energies.

have not been taken into account previously, contribute favorably to resolve the anomaly. The present calculation confirms the previous conclusion that the transverse interaction is important and should not be neglected in the NP calculation. However, there still remain large discrepancies between calculation and experiment.

In this regard, there are other kinds of QED corrections within the two-photon exchange processes, e.g., combined vacuum-polarization and nuclear-polarization correction (VP-NP) [17]. We have calculated the energy shift of muon bound states due to the combined VP-NP contribution along the lines with the method displayed in Ref. [17]. In the calculation, we have employed RPA wave functions instead of the collective model. They are summarized in Table II. The energy shift is quite large and it is about 33% of the NP

TABLE II. Combined vacuum-polarization and nuclear-polarization corrections (eV) in muonic ^{208}Pb.

State	$s_{1/2}$	$2s_{1/2}$	$2p_{1/2}$	$2p_{3/2}$	$3p_{1/2}$	$3p_{3/2}$	$3d_{3/2}$	$3d_{5/2}$
$\Delta E_{\text{VP-NP}}$	$+1547$	$+298$	$+219$	$+153$	$+71$	$+53$	$+4$	$+2$

energy for the $1s_{1/2}$ and $2s_{1/2}$ states, and about 10% for the other states. The VP-NP effect on the fine-structure splitting energies is also shown in Figs. 2(a) and 2(b) by black triangles. Combined VP-NP has an effect of moving black circles to black triangles along the line parallel to the shaded area. The effect of VP-NP may be interpreted as to increase the charge radius of a nucleus. The effect is unable to explain the $\Delta 2p$ and $\Delta 3p$ anomalies.

The $\Delta 2p$ anomaly might be attributed to a possible degeneracy between the muonic $2p$ levels and a 5.9 MeV 1^- nuclear excitation, which is not yet observed. Precision linewidth and intensity measurements of the x rays may be helpful to see if the anomaly has its origin in a resonance process involving the nuclear levels. A part of the discrepancies may come from the self-energy correction. In Ref. [4], they utilized the rather uncertain values for the Bethe logarithm and a $\alpha(Z\alpha)^2$ term [2]. There, the former is given by the mean value of the upper and lower bounds of the Bethe-Negele limits which are applicable only to the $1s$ muon [18], while the latter is given by the formula of Ref. [18] which is divided by a factor of 2.

In summary, we have calculated NP energy shifts in muonic ^{208}Pb utilizing the concept of effective photon propagators with nuclear-polarization insertions. The ladder, cross, and seagull terms of the two-photon exchange diagrams are evaluated in both the Feynman and Coulomb gauges. Gauge invariance was very well satisfied with the calculated NP energies.

Using these results we have analyzed fine-structure splitting energies of muonic ^{208}Pb because of the presence of the persisting discrepancies between experiment and calculation. The present nuclear-polarization energies could explain about half of the anomaly in the $\Delta 2p$ fine-structure splitting energy, while only one-fourth of the anomaly in the $\Delta 3p$ fine-structure splitting energy. The VP-NP contribution could neither solve the discrepancy, though the contribution was found to be comparable with nuclear-polarization energy.

[1] Y. Yamazaki *et al.*, Phys. Rev. Lett. **42**, 1470 (1979).
[2] G.A. Rinker, Comput. Phys. Commun. **16**, 221 (1979).
[3] M.V. Hoehn and E.B. Shera, Phys. Rev. C **30**, 704 (1984).
[4] P. Bergem *et al.*, Phys. Rev. C **37**, 2821 (1988).
[5] T.Q. Phan *et al.*, Phys. Rev. C **32**, 609 (1985).
[6] C. Piller *et al.*, Phys. Rev. C **42**, 182 (1990).
[7] G.A. Rinker and J. Speth, Nucl. Phys. A **306**, 360 (1978).
[8] Y. Tanaka and Y. Horikawa, Nucl. Phys. A **580**, 291 (1994).
[9] G.A. Rinker, Phys. Rev. A **14**, 18 (1976).
[10] R.K. Cole, Jr., Phys. Rev. **177**, 164 (1969).
[11] G. Plunien *et al.*, Phys. Rev. A **39**, 5428 (1989); **43**, 5853 (1991).
[12] G. Plunien and G. Soff, Phys. Rev. A **51**, 1119 (1995); **53**, 4614(E) (1996).
[13] A.V. Nefiodov *et al.*, Phys. Lett. A **222**, 227 (1996).
[14] A. Haga *et al.*, Phys. Rev. A **65**, 052509 (2002).
[15] J.L. Friar and M. Rosen, Ann. Phys. (N.Y.) **87**, 289 (1974).
[16] R. Rosenfelder, Nucl. Phys. A **393**, 301 (1983).
[17] L.N. Labzowsky *et al.*, J. Phys. B **29**, 3841 (1996).
[18] R.C. Barrett, Phys. Lett. B **28**, 93 (1968).